Transactions of KSAE, Vol. 34, No. 3, pp.355-363 (March, 2026)

pISSN 1225-6382 / eISSN 2234-0149
DOI http://dx.doi.org/10.7467/KSAE.2026.34.3.355

〈 Technical Paper 〉

A Simulation-Based Optimal Design Study for Enhancing the Torsional Stiffness of a Bus Body-in-White (BIW)

Sungyong Ha*

Joongbu University, Department of Smart Mobility engineering, Goyang-si, Gyeonggi 10279, Korea
(Received 6 January 2026 / Revised 22 January 2026 / Accepted 28 January 2026)

Abstract : Due to its long wheelbase and high cabin structure, a bus is inherently vulnerable to torsional loads. This study conducted a finite element analysis(FEA)-based simulation to propose an optimal design methodology for improving the torsional stiffness of the Body-in-White (BIW) structure of a large bus. The torsional response of a baseline BIW model was analyzed using Abaqus, and various reinforcement design alternatives were applied to evaluate stiffness and weight efficiency. The results showed that reinforcement of the lower floor and roof side rails was the most effective in enhancing stiffness. This study provides a foundation for lightweight and high-stiffness structural design in the early stages of bus body development.

Key words : BIW, Torsional stiffness, Roof rail, Floor frame, Cross member, Stiffness reinforcement

1. Introduction

Torsional stiffness of the vehicle body is a critical design factor that directly affects structural safety and dynamic performance during driving, and extensive research has been continuously conducted to improve it. In particular, commercial vehicles such as buses are subjected to significantly higher torsional loads than passenger cars due to their large body size and diverse loading conditions, making high-stiffness structural design essential.

Zhang and Tao[1] presented a systematic optimization procedure for bus body shape and dimensional design based on stiffness sensitivity analysis, demonstrating that FEM-based sensitivity methods can serve as practical lightweight design tools even for large-scale body structures. Zhao et al.[2] proposed a reliability evaluation methodology for bus body strength and stiffness based on probabilistic finite element analysis, and verified that a more realistic assessment of structural safety can be achieved by considering correlations among operating conditions. Boada et al.[3] experimentally demonstrated that lightweight design can be achieved while maintaining or improving torsional stiffness, providing an important foundation for subsequent analysis-based optimal design and reliability studies of bus body-in-white (BIW) structures.

In addition, Gauchía et al.[4] established the reliability of their proposed methodology by comparing and validating experimental results with finite element analysis outcomes for predicting the static and dynamic performance of bus body structures, thereby providing a basis for efficient structural performance evaluation in the early design stage. Zhong et al.[5] applied a multi-objective simultaneous topology-size optimization technique to a bus body frame to achieve weight reduction, torsional stiffness enhancement, and vibration performance improvement concurrently. This approach overcomes the limitations of conventional experience -based design and single-objective optimization, and proposes a high-performance, manufacturable bus body structural design strategy. Rooppakhun and Wichairahad[6] demonstrated that, in large bus body structural analysis, the accuracy of beam-element-based FEM can be significantly improved by incorporating joint flexibility while maintaining computational efficiency. Nguyen et al.[7] proposed an optimal design procedure that explicitly incorporates the ECE R66 rollover safety regulation as a

*Corresponding author, E-mail: hsy1396@joongbu.ac.kr

design constraint, while simultaneously considering rollover safety and lightweight design by selecting the thicknesses of major structural members as design variables.

Yang et al.[8] conducted finite element analysis on the body frame structure of a hydrogen fuel cell city bus to investigate structural behavior under major static loading conditions, and applied size optimization focusing on stress concentration regions to simultaneously achieve structural safety and weight reduction. Wang et al.[9] proposed a multilevel optimization methodology based on the Analytical Target Cascading (ATC) approach, in which the electric bus body is hierarchically decomposed into system- and subsystem-level models to simultaneously satisfy lightweight design, torsional stiffness, and modal performance requirements.

More recently, Taghizade et al.[10] comprehensively analyzed the bending stiffness, torsional stiffness, and modal characteristics of a bus body using finite element analysis, thereby identifying load transfer paths and structural weak points, and providing benchmark data for future structural optimization and lightweight design studies. Zhao et al.[11] integrated the BIW and stiffness test jig into a single unified structural model, contributing to improved reliability of BIW stiffness testing, enhanced correlation between experiments and simulations, and the establishment of a CAE-based validation framework for body structure optimal design.

Based on previous studies, this study develops a shell-based finite element model using actual bus BIW data and adopts an RBE2-based joint modeling approach to enable efficient analysis(for rapid analysis results). An optimal design procedure is then conducted to improve the torsional stiffness of the bus BIW structure. To enable rapid decision-making and practical applicability in the early design phase, reinforcement structures are classified into three categories: floor frame reinforcement, roof rail reinforcement, and cross-member reinforcement.

2. Characteristics of Bus Structures

Large buses, which are commercial vehicles designed for passenger transportation, are required to ensure both operational safety and structural durability. Among vehicle structures, the Body-in-White (BIW) plays a critical role in determining these performance characteristics. In particular, due to their long-wheelbase configuration, bus frames are structurally susceptible to torsional deformation under external loads. Such structural limitations can lead to degraded steering stability, fatigue failure, and increased interior noise.

Torsional stiffness is a key indicator representing these structural characteristics, as it quantifies the rotational rigidity between suspension mounting points and reflects the structure's resistance to torsional loads. However, in conventional bus design, improving torsional stiffness is often achieved at the expense of increased structural weight, which consequently results in reduced fuel efficiency and payload capacity. Therefore, there is a strong demand for optimized structural design methodologies that can enhance torsional stiffness while minimizing weight increase.

2.1 Structural Characteristics of Bus BIW

Compared to passenger cars, bus body structures are characterized by a long-wheelbase configuration of approximately 6–8 m, significant stiffness reduction caused by large openings such as doors and windows, the use of monocoque or semi-monocoque structural layouts, and a relative vulnerability to torsional deformation due to insufficient vertical symmetry of load-bearing members.

2.2 Definition and Calculation of Torsional Stiffness

Torsional stiffness is defined as the ratio of the applied torsional moment to the resulting angular deformation, and can be expressed as follows:

$$K_t = \frac{T}{\theta} \tag{1}$$

K_t : Torsional Stiffness(Nm/deg)

T : Applied Torque (Nm)

θ : Rotation Angle between Front Mounting Points (deg)

In general, opposite vertical loads (±F) are applied to the left and right front suspension points while the rear suspension is fixed to induce a torsional moment. The resulting rotational angle is then calculated from the relative displacement between the two points.

3. Analysis Model and Method

The vehicle illustrated in Fig. 1 corresponds to a

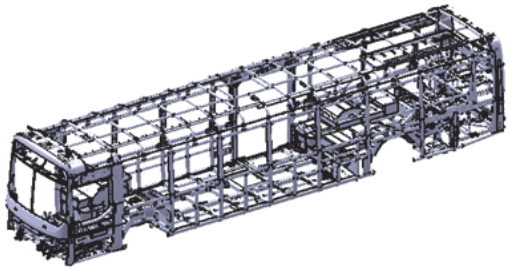

Fig. 1 Commercial bus model

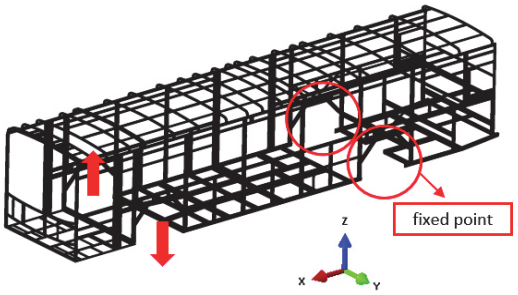

Fig. 2 Bus BIW model & boundary condition

commercially operated model in Korea, which is adopted as the baseline model for torsional stiffness analysis in this study.

3.1 Baseline Model

The analysis model used in this study (Fig. 2) is a simplified representation of the vehicle shown in Fig. 1, in which non-structural components such as doors, seats, and interior trim are excluded, and only the primary structural members are considered. The main structural components included in the model consist of cross members, floor structures, and roof rails.

3.2 Boundary Conditions and Loading Conditions

3.2.1 Boundary Conditions and Loading Conditions

A comparative structural response analysis was conducted by applying static torsional loading to the baseline BIW model and five reinforced design cases. The analysis was performed using linear static analysis in Abaqus. To induce torsion, opposite lateral forces were applied at the front mounting points, while the rear mounting points were fully constrained. The front and rear mounting regions were modeled by defining reference nodes at the tire center locations and rigidly connecting them to the surrounding structural nodes using RBE2 elements. The rigid-body assumption introduced by the RBE2 elements eliminates local compliance at the mounting interfaces, thereby ensuring stable load transfer and enabling accurate evaluation of the global torsional stiffness.

In addition, assuming a per-passenger load of 65 kg for a 32-passenger vehicle, the total applied load was calculated to be approximately 20,000 N. To simulate a static torsional test condition, this load was assumed to act in opposite directions on the left and right sides, resulting in an external load of approximately 10,000 N applied to each side. During the transition from the detailed BIW structure shown in Fig. 1 to the simplified analytical model in Fig. 2, the overall applied load was reduced to one-fifth by considering the structural simplification ratio resulting from the omission and idealization of detailed components. Accordingly, a final lateral force of 2,000 N was distributed to each side in opposite directions and applied at the front mounting regions. This loading configuration was designed to induce a pure torsional moment in the vehicle body, thereby enabling quantitative evaluation of the global torsional stiffness characteristics of the BIW structure.

The load determination method adopted in this study is based on a torsional stiffness evaluation using linear static

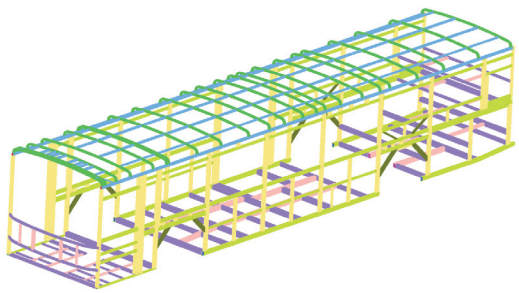

Fig. 3 Full bus finite element model

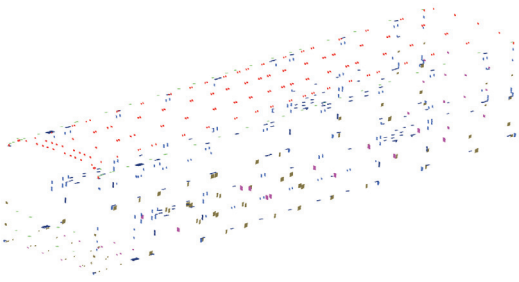

Fig. 4 Bus rigid welding RBE2

Table 1 Specifications of the bud vehicle

	Specification
Overall length	12,505 mm
Overall width	2,490 mm
Overall height	3,400 mm
Wheel base	6,200 mm
Passenger capacity	32

analysis. In such analyses, torsional stiffness is governed primarily by the load application locations and the relative distribution of left-right forces rather than by the absolute magnitude of the applied load. As long as the structural response remains within the elastic regime, the load-deformation relationship preserves linearity. Therefore, linearly scaling the reference load derived from actual vehicle conditions according to the structural simplification ratio represents an engineeringly sound approach that reasonably reproduces global structural behavior while ensuring computational efficiency.

3.2.2 Finite Element Analysis Model

The material properties of the vehicle body used in this study are summarized in Table 2, and the S4R element type was employed in the finite element model. In Abaqus, the S4R element is a shell element capable of efficiently and accurately representing the behavior of thin-walled structures, and it is widely used in large-scale structural analyses such as vehicle body-in-white (BIW) models. The S4R element is a four-node shell element with reduced integration, which uses a limited number of integration points and therefore offers excellent computational efficiency. As a result, it enables effective reductions in analysis time and computational resources even for vehicle body analyses consisting of several hundred thousand elements.

In addition, the S4R element allows convenient coupling with reinforcements, frames, spot welds, and RBE2 elements, making it possible to simplify the actual vehicle body structure while still effectively capturing its structural

Table 2 Material properties[2)]

	SAPH440
Density	7.85 kg/m^3
Young's modulus	206.8 GPa
Poisson's rate	0.29

Table 3 FE model information

Number of nodes	810,955
Number of elements	804,521
Average element length	10 mm

characteristics. For these reasons, it is commonly adopted as a standard element for analyses of body torsional stiffness, bending stiffness, and noise, vibration, and harshness (NVH). The analysis model information for the baseline design is presented in Table 3. To examine the potential for improving torsional stiffness, several reinforced design cases were applied and evaluated.

To ensure practical applicability and industrial relevance, the scope of the design modifications was deliberately constrained in this study. Specifically, changes in material properties and drastic alterations of cross-sectional geometries were excluded, as such modifications often lead to significant increases in manufacturing cost and may adversely affect production feasibility. Instead, the proposed reinforcement strategies were limited to local structural enhancements of existing members, allowing the effects of realistic and manufacturable design changes on torsional stiffness to be systematically evaluated.

3.3 Structural Design Variables

The reinforcement configurations were classified into three categories: floor frame reinforcement, roof rail reinforcement, and cross-member reinforcement. To evaluate the influence of reinforcement location, the designs were divided into the front and central regions of the body, excluding the fixed rear section.

Table 4 Design variables

Case	Improvements	Objective
Base	-	-
Case A	Additional floor reinforcements (center members)	Improve lower body stiffness
Case B-1	Roof rail cross-section change (60 × 40 → 60 × 60 mm)	Enhance upper body stiffness
Case B-2	Roof rail cross-section change (60 × 40 → 80 × 40 mm)	Enhance upper body stiffness
Case C-1	Increase number of cross-members (front position)	Improve overall torsional stiffness
Case C-2	Increase number of cross-members (center position)	Improve overall torsional stiffness

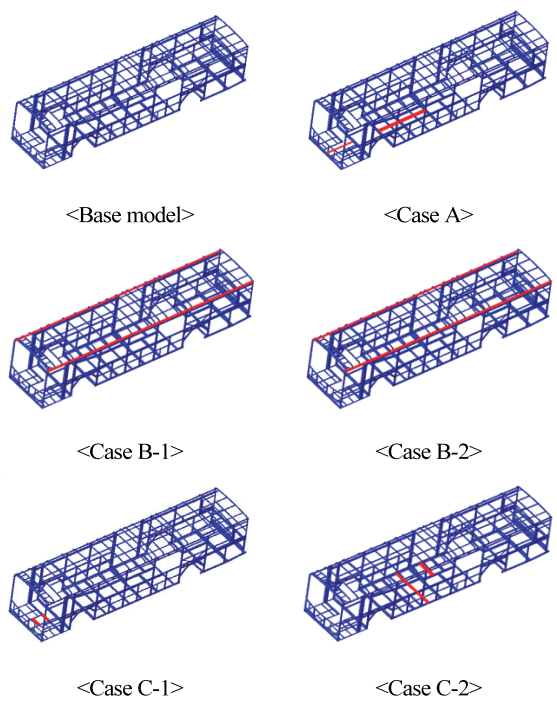

Fig. 5 Design change location

In Case A, the floor structure was reinforced with the objective of enhancing lower-body stiffness. In Cases B(1) and B(2), the cross-sectional geometry of the roof rails on both sides was modified to improve upper-body stiffness. In addition, to assess the effect of cross-sectional configuration, the reinforcements were designed by distinguishing between horizontal and vertical directional enhancements. Finally, in Cases C(1) and C(2), overall structural stiffness was improved through cross-member reinforcement.

The baseline design and the proposed reinforced configurations are summarized in Table 4, and the locations of the modified regions are illustrated in Fig. 5.

4. Results and Discussion

4.1 Comparison of Torsional Stiffness

The changes in torsional stiffness for each proposed design case compared to the baseline model are summarized as follows.

For Case A, the torsional stiffness increased to 11,690 Nm/deg, representing an improvement of approximately 3.1 %, while the structural weight increased by about 1.7 %.

In Case B-1, the torsional stiffness decreased to 11,157 Nm/deg, corresponding to a reduction of approximately 1.6 %, with a weight increase of about 1.0 %.

Table 5 Stiffness results

Case	Stiffness (Nm/deg)	Weight (kg)	Stiffness/Weight ratio
Base	11,340	1,684	6.73
Case A	11,690	1,712	6.83
Case B-1	11,157	1,702	6.56
Case B-2	12,004	1,702	7.05
Case C-1	11,355	1,694	6.70
Case C-2	11,673	1,699	6.87

In contrast, Case B-2 exhibited an increase in torsional stiffness to 12,004 Nm/deg, showing an improvement of approximately 5.9 %, while the weight also increased by approximately 1.0 %.

For Case C-1, the torsional stiffness slightly increased to 11,355 Nm/deg, corresponding to an improvement of approximately 0.1 %, accompanied by a weight increase of about 0.6 %.

Finally, Case C-2 showed a torsional stiffness of 11,673 Nm/deg, representing an improvement of approximately 2.9 %, with a corresponding weight increase of approximately 0.9 %.

Except for Case B-1, most reinforcement configurations demonstrated positive effects on torsional stiffness. From the overall comparison, it can be concluded that transverse reinforcement strategies are more effective than longitudinal reinforcements in enhancing the torsional stiffness of the bus body structure. The difference between Cases B-1 and B-2 indicates that the rectangular cross-section used in Case B-2 provides higher stiffness than the square cross-section in Case B-1, due to its larger second moment of area about the vertical axis.

The variations in torsional stiffness, structural weight, and stiffness-to-weight ratio resulting from the analysis are summarized in Table 5, and the corresponding analysis results are illustrated in Fig. 6.

4.2 Stress Analysis

The maximum stress of the baseline model was found to be 320.7 MPa, occurring at the central region of the rear door frame. Case A exhibited a similar stress distribution, with a maximum stress of 320.5 MPa occurring at the same location. In Case B-1, a slight increase in maximum stress was observed, reaching 324.2 MPa, and the peak stress also appeared at the same region.

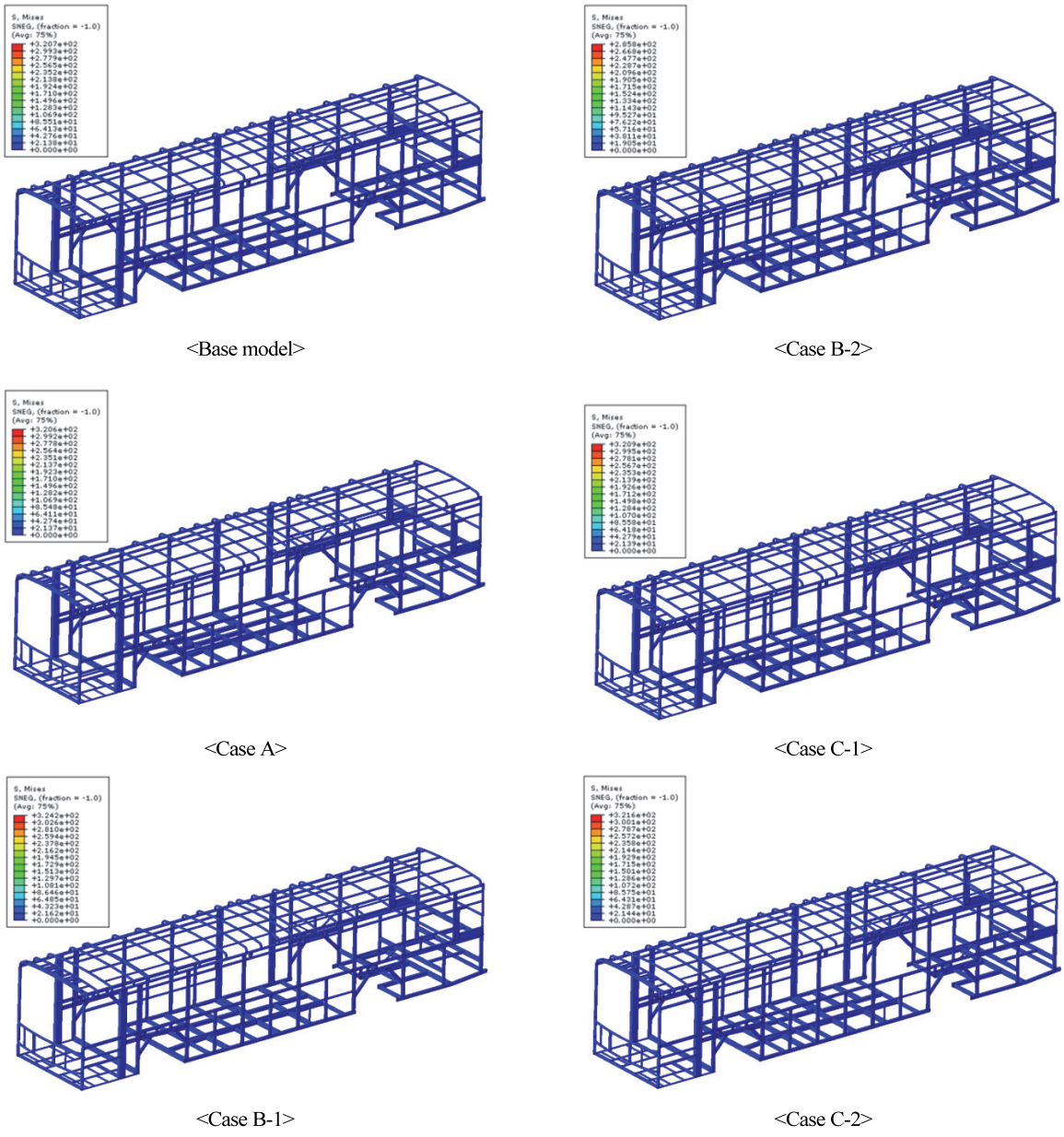

<Base model> <Case B-2>

<Case A> <Case C-1>

<Case B-1> <Case C-2>

Fig. 6 Stress results

In contrast, Case B-2 showed a significant reduction in maximum stress to 285.8 MPa, corresponding to an approximate 11 % decrease compared to the baseline model. Moreover, the location of the maximum stress shifted from the central region of the rear door frame to the upper region of the structure. For Case C-1, the maximum stress was 320.9 MPa and occurred at the same location as in the baseline model. Similarly, Case C-2 exhibited a maximum stress of 321.6 MPa at the same region, indicating a negligible change in stress distribution.

4.3 Deformation Analysis

Since opposite directions of vertical loads were applied to the left and right sides, the resulting displacements also appeared in both positive and negative directions. The displacement results were summarized in Table 6 based on the maximum deviation values along each axis. Similar to the torsional stiffness results, most reinforced cases exhibited an overall reduction in displacement compared to the baseline model.

However, Case B-1 showed an increasing trend in

Table 6 Stress results

Case	Stress (MPa)	Decrease rate
Base	320.7	-
Case A	320.5	-0.07 %
Case B-1	324.2	+1.09 %
Case B-2	285.8	-10.9 %
Case C-1	320.9	+0.06 %
Case C-2	321.6	+0.28 %

Table 7 Displacement results (Unit: mm)

Case	X-axis	Y-axis	Z-axis
Base	4.988	25.98	33.91
Case A	4.894	25.16	32.95
Case B-1	6.774	26.17	38.04
Case B-2	4.048	24.72	31.09
Case C-1	2.311	25.94	32.12
Case C-2	4.902	25.21	32.97

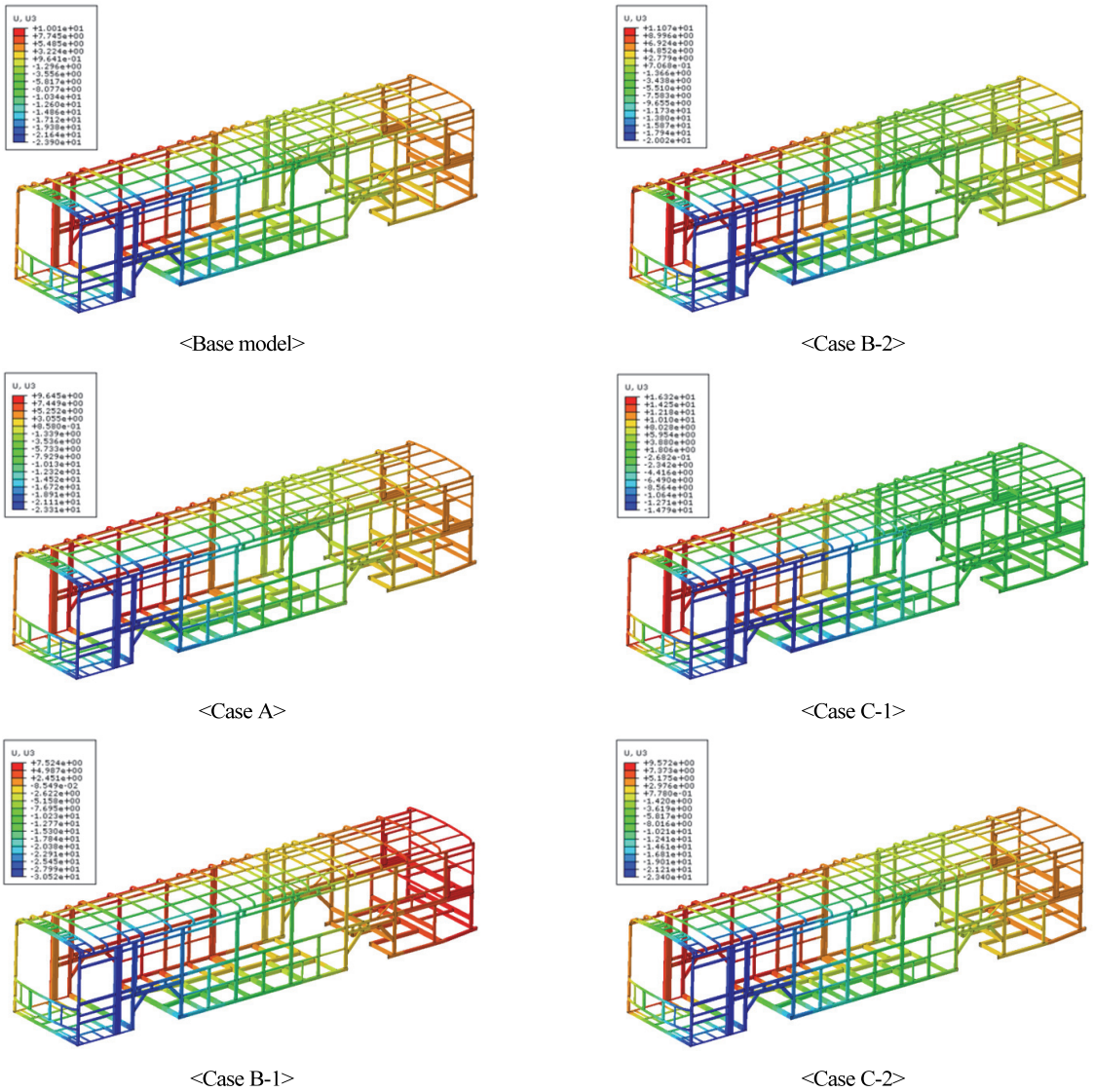

Fig. 7 Displacement results

deformation in all directions, which is consistent with the previously observed reduction in torsional stiffness. In contrast, Case B-2 demonstrated a uniform reduction in displacement across all directions, in agreement with its improved stiffness performance. Additionally, Case C-1 showed a noticeable reduction in displacement particularly

along the x-axis (vehicle longitudinal direction). This behavior is attributed to the reinforcement effect of the cross members located in the front region where torsional loading was applied.

Among these results, the displacement distribution in the z-axis direction is illustrated in Fig. 7.

4.4 Convergence Check

To ensure the reliability of the numerical results, a convergence assessment was conducted. All analyses in this study were performed using linear static analysis in Abaqus, and nonlinear effects, including material nonlinearity, geometric nonlinearity, and contact nonlinearity, were not considered. Accordingly, the global stiffness matrix was stably constructed for each analysis case, and it was confirmed that the residual forces decreased within the prescribed tolerance limits during each load step.

In addition, identical mesh densities and analysis conditions were applied to both the baseline BIW model and all reinforced design cases to ensure consistency in convergence behavior. For all cases, displacement and reaction force responses exhibited stable convergence throughout the iterative solution process. Furthermore, mesh refinement studies indicated that additional mesh densification resulted in negligible changes in the global torsional stiffness, thereby confirming mesh independency. Based on these convergence evaluations, the comparative torsional stiffness results obtained in this study are numerically stable and can be regarded as reliable.

5. Conclusion

In this study, structural design strategies for improving the torsional stiffness of a BIW were evaluated using Abaqus. Simulation-based analyses were conducted for various reinforced design configurations, and the results demonstrated that most of the proposed reinforcement strategies were effective in enhancing torsional stiffness. Among them, Case B-2, which increases the second moment of area of the roof rail cross-section, exhibited the most effective improvement in torsional stiffness while maintaining superior weight efficiency.

The main conclusions of this study are summarized as follows:

Reinforcement of the floor frame, roof rails, and cross members was found to be effective in improving torsional stiffness.

Increasing the vertical dimension of the roof rail cross-section provided the greatest stiffness improvement relative to the added weight.

An optimal design configuration (Case B-2) was identified that achieves torsional stiffness enhancement while minimizing the increase in overall structural weight.

In future work, experimental validation and topology optimization techniques will be incorporated to achieve more precise and optimized structural designs.

Reviews

This research was supported by the 2025 research fund of Joongbu University.

References

1) X. Zhang and Z. Tao, “A Study on Shape Optimization of Bus Body Structure Based on Stiffness Sensitivity Analysis,” Proceedings of the IEEE, pp.1-6, 2009.
2) D. Zhang, T. Zhang, G. Zhang and W. Zhao, “Structural Reliability Analysis of Bus Body in Consideration to the Correlation of Working Conditions,” Proceedings of the International Conference on Measuring Technology and Mechatronics Automation (ICMTMA), pp.133-136, 2009.
3) A. Gauchía, V. Díaz, M. J. L. Boada and B. L. Boada, “Torsional Stiffness and Weight Optimization of a Real Bus Structure,” Int. J. Automotive Technology, Vol.11, No.1, pp.41-47, 2010.
4) A. Gauchía, E. Olmeda, M. J. L. Boada, B. L. Boada and V. Díaz, “Methodology for Bus Structure Torsion Stiffness and Natural Vibration Frequency Prediction Based on a Dimensional Analysis Approach,” Int. J. Automotive Technology, Vol.15, No.3, pp.451-461, 2014.
5) H. Zhong, Y. Zhang, H. Li and Z. Chen, “Multi-objective Topology and Sizing Optimization of Bus Body Frame,” Structural and Multidisciplinary Optimization, Vol.54, No.2, pp.397-412, 2016.
6) S. Rooppakhun and J. Wichairahad, “The Strength Analysis of a Bus Superstructure Based on the Accuracy Improvement of T-Junction Flexible Joint Stiffness,” International Journal of Engineering &Technology, Vol.7, No.3.24, pp.62-67, 2018.
7) T. -T. Nguyen, C. -T. Nguyen, V. -S. Nguyen and D.

-N. Nguyen, “Optimal Design for Body Structure of Coach Bus to Satisfy Rollover Collision Safety Based on ECE R66 Standard,” Proceedings of the International Conference on Automotive and Mechanical Engineering, pp.1-12, 2023.

8) X. Yang, Z. Li, H. Zhang, Y. Liu and W. Chen, “Finite Element Analysis and Optimization of Hydrogen Fuel Cell City Bus Body Frame Structure,” Applied Sciences, Vol.13, No.8, pp.1-17, 2023.

9) X. Wang, Y. Li, H. Zhang and Z. Chen, “Lightweight Design of an Electric Bus Body Structure with Analytical Target Cascading,” Frontiers of Mechanical Engineering, Vol.18, No.3, pp.1-14, 2023.

10) Z. Taghizade, M. Yaghoobian and J. Marzbanrad, “Torsional and Bending Stiffness and Modal Analysis of a Bus Structure,” Automotive Science and Engineering, Vol.14, No.3, pp.4439-4448, 2024.

11) Z. Hu, S. Mo, H. Liu and F. Mo, “Optimization Design of Body-in-White Stiffness Test Rig Based on the Global Adaptive Algorithm of the Hybrid Element Model,” Applied Mechanics, Vol.6, No.1, p.18, 2025.